Journal of Magnetism and Magnetic Materials 591 (2024) 171748

Contents lists available at ScienceDirect

Journal of Magnetism and Magnetic Materials

journal homepage: www.elsevier.com/locate/jmmm

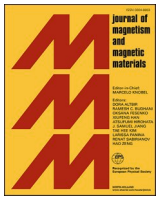

Influence of coating on peroxidase-like activity of magnetic nanoparticles

I. Khmara [a,*], I. Antal [a], A. Jurikova [a], M. Kubovcikova [a], V. Zavisova [a], V. Girman [b], M. Koneracka [a]

[a] Institute of Experimental Physics, Slovak Academy of Sciences, Watsonova 47, 040 01 Kosice, Slovakia
[b] Institute of Physics, Faculty of Sciences, Pavol Jozef Safarik University in Kosice, Park Angelinum 9, 041 54 Kosice, Slovakia

ARTICLE INFO

Keywords:
Magnetic nanoparticles
Chitosan
Peroxidase-like activity
Hydrogen peroxide

ABSTRACT

Chitosan stabilized iron oxide magnetic nanoparticles (Chit-MNPs) were prepared with the theoretical Chit/Fe_3O_4 weight ratios equal to 0.5, 1, 2, 3 w/w and characterized by different techniques. The effect of various Chit/Fe_3O_4 weight ratios on the samples' hydrodynamic diameter, zeta potential, and isoelectric point was studied by the dynamic light-scattering method. Using TEM analysis, the average magnetic core size was found to be ranging from 6 nm to 9 nm. The obtained results are comparable to those from magnetic measurements. The magnetic measurements confirmed successful chitosan coating on MNPs by means of the decrease in saturation magnetizations from 69.2 emu·g^{-1} for unmodified MNPs to 66.6, 65.9, 65.5 and 65.2 emu·g^{-1} for Chit-MNPs at different ratios of Chit/MNPs 0.5, 1, 2, and 3. TGA was used to quantify the amount of chitosan adsorbed on MNPs surface – the max. amount was 0.045 mg chitosan/mg MNPs. The peroxidase-like catalytic activity of unmodified MNPs and chitosan Chit-MNPs in present of a substrate such as N,N-diethyl-p-phenylenediamine sulfate salt (DPD) and hydrogen peroxide was studied. The results confirmed the peroxidase-like activity of samples, – they catalytically oxidise substrate DPD by H_2O_2 to produce a typical colour reaction. The chitosan coating was found to slightly decrease catalytic activity compared to MNPs at pH 7.4. Despite the fact, these findings can be useful for creating sets of MNPs and Chit-MNPs samples possessing predefined peroxidase-like activity and could be applied for chromogenic reactions in the future.

1. Introduction

Today, nanoscale materials are of great scientific and technical interest in various fields [1]. Iron oxide magnetic nanoparticles (MNPs) such as Fe_3O_4 (magnetite) and γ-Fe_2O_3 (maghemite) as a type of nanoscale materials are of great interest due to their extremely small size, specific chemical, physical and biological properties and large surface area per unit volume. Therefore, iron oxide MNPs are receiving considerable attention in biological applications such as magnetic resonance imaging [2,3], magnetic hyperthermia [4,5], and targeted drug delivery [6,7]. Recently, it was also reported that iron oxide MNPs could function like an artificial peroxidase[8]. The significance of this finding is justified by the fact that iron oxide MNPs are much more stable and have almost unchanged catalytic activity over a wide range of temperatures and pH compared to natural enzymes. Another important feature is that natural peroxidase enzymes are difficult to produce in large quantities since they are prone to proteolytic degradation, while iron oxide MNPs can be easily synthesized in large volumes and at relatively low cost [9]. These facts allow iron oxide MNPs to be used as natural peroxidase enzymes or to replace natural peroxidase enzymes in applications based on the detection of hydrogen peroxide [10,11]. Moreover, iron oxide MNPs can be utilized in bioassays and biomedical applications [8,12,13]. Since iron oxide MNPs have intrinsic peroxidase-like activity with catalytic behavior similar to horseradish peroxidase (HRP) [8] (i. e., they possess mechanisms similar to natural enzymes), this enables their wide use for both diagnostic and therapeutic purposes (anti-bacterial and cancer therapy). Moreover, HRP contains Fe^{3+} or Fe^{2+} ions in their active sites (just like iron oxide MNPs), which catalyze the oxidation of organic substances in the presence of H_2O_2. Such catalytic process involves Fenton reactions (see equations (1) and (2) which generate hydroxyl radicals (•*OH*) [14].

$$Fe^{2+} + H_2O_2 \rightarrow Fe^{3+} + \bullet OH + OH^- \quad (1)$$

$$Fe^{3+} + H_2O_2 \rightarrow Fe^{2+} + \bullet OOH + H^+ \quad (2)$$

To detect the peroxidase-like activity of nanoparticles in a reaction,

* Corresponding author.
E-mail address: khmara@saske.sk (I. Khmara).

https://doi.org/10.1016/j.jmmm.2024.171748
Received 31 October 2023; Received in revised form 22 December 2023; Accepted 13 January 2024
Available online 17 January 2024

generally both the consumption of hydrogen peroxide and the formation of the oxidized substrate are examined. For this purpose, colorimetric and fluorescence measurements are usually used as an analytical detection tool. They are based on the fact that peroxidase catalyzes the oxidation of certain substrates to produce a characteristic color in the presence of hydrogen peroxide [15,16]. The most commonly used peroxidase substrates are 3,3,5,5-tetramethylbenzidine (TMB), o-phenylenediamine (OPD), ABTS, and 3.3′-diaminobenzidine (DAB). Upon peroxidation, TMB is oxidized into oxTMB, producing a blue color in the solution. Similarly, OPD is oxidized into the oxidized-OPD, which has a yellow color. For example, Gao *et al.* [8] tested Fe_3O_4 magnetic nanoparticles which catalyzed the oxidation of three peroxidase substrates, TMB and OPD and showed that Fe_3O_4 magnetic nanoparticles had a lower Michaelis constant for TMB than HRP, despite the HRP has a higher affinity to the substrate H_2O_2. Tested with TMB, Fe_3O_4 nanoparticles showed a higher catalytic activity than HRP. Similar to HRP, the catalytic activity of Fe_3O_4 nanoparticles is dependent on pH, temperature, and H_2O_2 concentration [8]. Wei *et al.* [17] demonstrated that in the presence of H_2O_2, nano-Fe_3O_4 catalyzed the oxidation of the peroxidase substrate, 2,2́-azino-bis(3-ethylbenzothiazoline-6-sulfonic acid) diammonium salt (ABTS), and also suggested that nano-Fe_3O_4 can be used in a colorimetric method for detection of H_2O_2. In addition, Wei *et al.* [17] also determined that nano-Fe_3O_4 can serve as a sensitive and selective method for glucose detection. Furthermore, there are some works on the synthesis of iron oxide nanoparticles (IONPs) coated with different coating agents. IONPs were synthesized and their peroxidase-like activity was evaluated using glucose detection as a model system for determination [9] and glutathione [18]. It was suggested also [9], that MNPs can be applied in colorimetric determination of glucose in low concentration for detection of diabetes mellitus in patients tear fluid. As a model, hydrogen peroxide produced from oxidation of glucose-by-glucose oxidase was measured to indirectly measure glucose. The drugs with various beneficial effects can be loaded into chitosan modified MNPs. Hussein-Al-Ali *et al.* [19] studied ampicillin loaded chitosan MNPs nanocomposite and determined their antibacterial and antifungal properties, as well as antimycobacterial effects. In addition, the fact that the acceleration of the Fenton reaction generates reactive oxygen species can be used to induce the death of cancer cells [20]. The findings suggest that coating on IONPs can improve and lower their peroxidase-like activity.

Therefore, in this work, we aimed to prepare biocompatible MNPs having peroxidase-like activity and fulfil the main requirements for nanoparticles used in biology and medicine such as low toxicity, biocompatibility, biological degradation and the ability to be excreted from the body naturally. Chitosan was selected due to its biocompatibility, biodegradability, immuno-stimulating features, and high chemical reactivity leading to its extensive usage in a variety of biomedical and bioengineering applications [21]. The presence of both hydroxyl and amine residues in the chitosan monomer unit enhances the specific interaction of chitosan macromolecules with the surface of metal oxide MNPs and provides the stability of suspensions at low polymer concentrations. Next, we focused on studying the effect of the chitosan coating on the ability of MNPs to function as an artificial peroxidase. It is well known that MNPs can provide hydrogen peroxide-based oxidation of a substrate such as N,N-diethyl-p-phenylenediamine sulfate salt (DPD) to the radical cation $DPD^{\cdot+}$, which gives a persistent purple colour with absorption at 551 nm [22]. Therefore, it was important to study the effect of chitosan amount adsorbed on the surface of MNPs on peroxidase-like activity for this type of substrate. To confirm the peroxidase-like activity for Chit-MNPs, time dependency of DPD oxidation in the presence of constant concentration of MNPs (0.05 mg/mL of Fe_3O_4) has been studied by various concentrations of hydrogen peroxide.

2. Materials and methods

2.1. Chemicals

All chemicals used in this work were of analytical grade and used as received from manufacturer/provider without further purification. The following chemicals were used: iron (II) chloride tetrahydrate ($FeCl_2{\cdot}4H_2O$) from Merck, iron (III) chloride hexahydrate ($FeCl_3{\cdot}6H_2O$), hydrogen peroxide (H_2O_2, 30 %), chitosan (Chit) with low molecular weight (50–190 kDa and 75–85 % deacetylation degree), N,N-diethyl-p-phenylenediamine sulfate salt (DPD), sodium hydroxide (NaOH) from Sigma-Aldrich, acetic acid ($C_2H_4O_2$, 99 wt%), ammonium hydroxide solution (NH_4OH, 25 %), sodium phosphate dibasic dihydrate ($Na_2HPO_4{\cdot}2H_2O$) and sodium phosphate monobasic monohydrate ($NaH_2PO_4{\cdot}H_2O$) from Slavus (Slovakia). All solutions were prepared with ultrapure water.

2.2. Preparation of chitosan modified magnetic nanoparticles

2.2.1. Synthesis of magnetic nanoparticles by co-precipitation method

The magnetic Fe_3O_4 nanoparticles were synthesized by a chemical co-precipitation method using ferric and ferrous salts at a molar ratio of 2:1 in an alkali medium. Briefly, the mixture of Fe^{2+} and Fe^{3+} aqueous solutions was filtered to remove insoluble residues and then 4.5 % NH_4OH with dripping rate of dissolved ammonium at 6.8 mL/min was added at room temperature with constant stirring (>1000 rpm) to produce a black magnetite precipitate. The precipitate was washed three times by magnetic decantation using deionized water to remove salt residues. Finally, washed magnetite nanoparticles were uniformly suspended in the demineralized water and their concentration in the suspension was estimated by gravimetric analysis. The prepared suspension was designated with the name “MNPs”.

2.2.2. Preparation of chitosan-coated magnetic nanoparticles

The chitosan surface modification of MNPs was carried out in the following steps. First, 0.5 % w/v chitosan solution was prepared by dissolution of 0.5 g of chitosan to make up100 mL of 2 % aqueous acetic acid solution. Next, the constant volume of chitosan solution with the chitosan concentration ranging from 0.68 to 4.05 mg/mL was added to the aqueous suspension of the MNPs with constant Fe_3O_4 concentration equal to 1.35 mg/mL to form a dispersion with the theoretical Chit/Fe_3O_4 weight ratios equal to 0.5, 1, 2, 3 w/w. Then, the samples were diluted with ultrapure water to the final volume of 200 mL. Next, the formed solutions were incubated in a horizontal thermomixer (BioShake iQ) for 2 h at 95 °C and 350 rpm. Finally, the samples were ultracentrifuged at 55,000 rpm for 1 h at 4 °C to remove unbound chitosan and at the same time to increase the concentration of the prepared chitosan modified magnetic nanoparticles (Chit-MNPs). Having removed the supernatants, the sediments were dispersed in ultrapure water thoroughly and collected to subsequently produce the Chit-MNPs.

2.3. Instrumentation

The morphology and microstructure of unmodified MNPs and chitosan-coated MNPs were studied using transmission electron microscopy (TEM). For TEM analysis, the samples were diluted in distilled water and ultrasonicated. A droplet of the water-diluted colloidal dispersion was deposited on a copper grid coated with lacey carbon film. The grids were dried in a vacuum. The prepared samples were observed employing a transmission electron microscope (TEM, JEOL TEM 2100F UHR microscope) equipped with a Schottky FEG source and operated at 200 kV acceleration voltage. For imaging of sample nanoparticles, both STEM-BF and TEM-BF modes were used. The average size distribution was determined by manual image analysis evaluating at least 200 particles for each sample.

To determine the mean size and particle size distribution, the

samples were measured by the dynamic light scattering (DLS) method using a Zetasizer NanoZS (Malvern Instruments, Malvern, UK). DLS evaluates the fluctuations of scattered light intensity diffracted from nanoparticles undergoing steady Brownian motion in the suspension. The electrokinetic zeta potentials of the samples were measured by Doppler electrophoretic measurements with a scattering angle of 173° at 25 ± 0.1 °C the same instrument.

The complementary technique used to determine the size distribution of the Chit-MNPs with different weight ratios of $Chit_x$/MNPs (x = 0.5, 1, 2, 3) was the CPS Differential Centrifugal Sedimentation. The DC24000 UHR disk centrifuge (CPS Instruments, Inc., Prairieville, LA, USA) was used to measure particle size distributions using sedimentation, indicating that Chit-MNPs were settled in a fluid under a gravitational field according to Stokes' Law and sedimentation velocity increased as the square of the particle diameter.

The Fourier Transform Infrared Spectroscopy (FTIR) spectra of chitosan, the magnetic nanoparticles (MNPs), Chit-MNPs with different weight ratios of $Chit_x$-MNPs (x = 0.5, 1, 2, 3), and physical mixture of chitosan and MNPs samples were collected using a Vertex 80-v instrument (Bruker, Bremen, Germany) in transmission mode within the range of 530 cm^{-1} to 4000 cm^{-1} with a resolution of 4 cm^{-1}. For these studies all samples were washed with ultrapure water before being lyophilized and freeze-dried in a lyophilizer at − 52 °C.

Magnetic measurements of the $M(H)$ curves of the samples were carried out with a SQUID magnetometer (MPMS 5XL, Quantum Design, Darmstadt, Germany) at room temperature.

Thermogravimetric analysis (TGA) was used to show thermal decomposition and to estimate chitosan content in the prepared Chit-MNPs. TG measurements were performed for washed and dried samples under the air atmosphere with a rate of 10 °C·min^{-1} from the room temperature up to 700 °C using TGDTA Setaram SETSYS 16 analyzer.

Absorption measurements were performed on a UV/VIS spectrometer (Specord 40, Analytik, Jena, Germany).

2.4. Measurement of peroxidase-like activity

Peroxidase-like activity was determined using 1 M hydrogen peroxide and 12.5 mM DPD as substrates [23]. DPD was obtained by dissolving DPD powder in ultrapure water, and stored in the dark vial before its use. The total reaction volume of 1 mL contained 0.05 M phosphate buffer with pH 7.4, 1.0 M H_2O_2, 12.5 mM DPD, and MNPs or Chit-MNPs with different ratios of Chit/ MNPs (0.5, 1, 2, and 3 w/w). After mixing of all components, the purple colour appeared and developed as reactions proceeded. This process was monitored at room temperature using a UV/VIS spectroscopy. Catalytic parameters were determined by fitting the steady-state reaction rates data to the Michaelis-Menten equation:

$$v = \frac{1}{V_{max}} + \frac{K_M}{V_{max}[S]} \tag{3}$$

where v is the initial velocity, V_{max} is the maximal reaction velocity, K_M is the Michaelis-Menten constant, $[S]$ is the concentration of substrate.

3. Results and discussion

3.1. Characterization of chitosan modified magnetic nanoparticles

To verify the successful preparation of chitosan modified magnetic nanoparticles, a series of measurements including TEM, DLS, DCS, SQUID magnetometer, TGA and FTIR were carried out. TEM and HRTEM images were also acquired to assess the surface morphology of

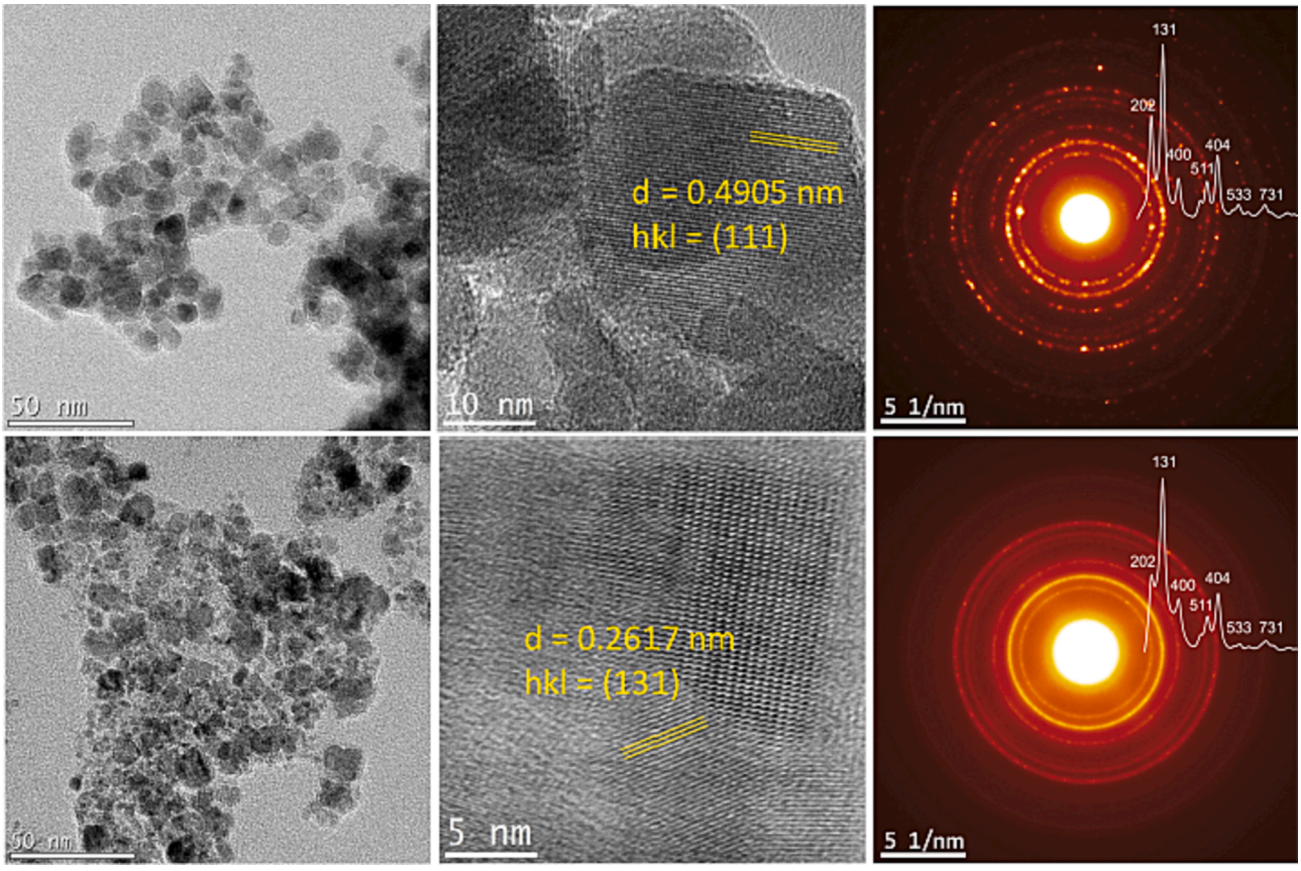

Fig. 1. TEM, HRTEM images, and electron diffraction patterns of unmodified magnetic nanoparticles (a-c) and chitosan modified magnetic nanoparticles Chit-MNPs-C (d-f).

the Fe_3O_4 and Chit-MNPs nanostructures (Fig. 1). According to HRTEM images, the synthesized nanoparticles were quasi-spherical with an average size of 6 – 9 nm (Fig. 1a, b, d, f). Measured interplanar distances in HRTEM images were 0.4905 nm for MNPs (Fig. 1c), and 0.2617 nm for Chit-MNPs-C (Fig. 1f). The same distances were found in reciprocal space represented by electron diffraction patterns. Distances correspond to the (1 1 1), and (1 3 1) lattice plane system of the Fe_3O_4 phase (SG: 227, Fd-3 m, cubic crystal system). The Fe_3O_4 phase was confirmed by analysis of all diffraction rings. Before processing, the electron diffraction patterns were radially integrated. The obtained diffraction profiles are embedded in diffraction patterns (Fig. 1c, f). The fact that nanoparticles were quasi-spherical with an average core size ranging from 6 nm to 9 nm indicates their excellent catalytic ability, as MNPs with smaller sizes and larger specific surface areas are reported to show higher catalytic activity [8].

Hydrodynamic size distributions measured by DLS and DCS methods are summarized in Table 1. As seen, the increase in D_{DLS} as well as in D_{DCS} was observed with the Chit/MNPs weight ratios increasing, indicating Chit adsorption on MNPs surface (Fig. 2 (left)). The reduction of diameter of Chit-MNPs samples compared to the value for unmodified MNPs is caused by the role of chitosan as a stabiliser.

The successful coverage of MNPs by chitosan was also confirmed by measuring each sample's zeta potential (ZP) as a function of pH and by identifying the pH where the ZP value crosses zero (Isoelectric point IEP). Fig. 2 (right) shows the IEP of unmodified MNPs, four samples of Chit-MNPs with different theoretical Chit/MNPs weight ratios, and pure Chit. The more chitosan molecules are adsorbed, the more IEP moves from the IEP of the MNPs (pH 6.5) toward the IEP of the pure Chit (pH ~ 9.2) correlating with the degree of surface coverage of the nanoparticle with Chit.

The necessary condition for the biomedical application of the suspension of MNPs is the maintenance of its colloidal stability. As ZP is commonly used to predict and control dispersion stability, we measured the ZP of the MNPs and Chit-MNPs samples in water. The results are summarized in Table 1. It can be seen that modification of MNPs with chitosan resulted in an increase of ZP from +15.5 up to +36.4 mV, suggesting that Chit was adsorbed on MNPs surface. Moreover, the ZP above +30.8 mV indicates good stability of the samples with Chit/MNPs = 2 w/w.

The magnetic properties of the prepared samples were investigated and are presented in Fig. 3. The SQUID magnetometer was used to characterize the magnetization M of the MNPs and Chit-MNPs samples as a function of the external applied field H. The magnetization curve at room temperature in Fig. 3 (left) demonstrates the magnetization saturation M_S of ~69.2 emu·g^{-1} for MNPs and 66.6, 65.9, 65.5 and 65.2 emu·g^{-1} for Chit-MNPs at different ratios of Chit/ MNPs 0.5, 1, 2, and 3. The decrease of the saturation magnetization of the modified samples with increasing Chit/MNPs weight ratios in comparison to unmodified MNPs is caused by the coating process, i.e., by the formation of a magnetic dead layer by chitosan. Next, the experimental results from $M(H)$ measurements were fitted by the Langevin function:

$$M = M_S \int_0^{\infty} L\left(\frac{\mu H}{kT}\right) f(V) d(V)$$

where M is the specific magnetization, M_S the specific saturation magnetization, μ is the magnetic moment of a single particle at particular temperature, k is the Boltzman constant and $f(V)$ is volume distribution of particle size. To perform the calculations for particle size distribution, we have used the simplifying assumption that particles are spherical, i.e. $V = \pi D^3/6$, with a log-normal distribution of D values,

$$f(D) = \frac{1}{\sigma D\sqrt{2p}} expexp\left(-\frac{(lnD - \epsilon)^2}{2\sigma^2}\right.$$

where D is the particle diameter, and ε and σ are the mean and standard deviation of ln D, respectively [24]. As seen in Fig. 3 right, calculated D_{MAG} are approximately the same and are close to diameters estimated from the TEM measurements.

The thermogravimetric curves obtained for the samples of the unmodified MNPs and Chit-MNPs with different ratio of Chit to MNPs are presented in Fig. 4 (left).

The initial weight loss due to adsorbed water evaporation can be seen for all investigated samples. After that, the unmodified MNPs were stable in the investigated temperature interval while pure Chit decomposes in several stages up to the temperature of about 600 °C [2,4].

For Chit-MNPs samples, two main decomposition stages were observed – the first one up to about 250 °C and the second one up to about 400 °C. During next heating the Chit-MNPs samples show no weight loss during the heating up to about 700 °C. Their total weight loss increased from 8.2 to 9.8 % with increasing input Chit/MNPs ratio.

Since free chitosan is fully decomposed at the temperature of 700 °C, the MNPs in Chit-MNPs samples should remain as a residue, hence amount of chitosan adsorbed on MNPs can be determined as a difference between Chit-MNPs a MNPs residues. The adsorption of chitosan as an effect of the input Chit/MNPs ratio is displayed in Fig. 4 (right). The saturation tendency can be seen suggesting that maximally 0.045 mg of chitosan can be bounded onto 1 mg MNPs. The amounts of Chitosan bounded on MNPs in mg Chit/ mg MNPs for the investigated samples are summarized in Table 1.

FT-IR spectra of pure chitosan, Chit-MNPs-C, unmodified MNPs and physical mixture (PM) of chitosan and MNPs are shown in Fig. 5 (left). The main characteristic bands for chitosan appeared at 3355 cm^{-1} (O–H and N–H stretching vibrations), 2873 cm^{-1} (C–H stretching vibrations), 1646 cm^{-1} (N–H bending vibrations) and 1060 cm^{-1} (C–O–C stretching vibrations) [2,25,26]. Additionally, the peak at 544 cm^{-1} (Fig. 5c (left)) is attributed to the Fe-O group [27,28]. The characteristic peaks of MNPs at 554 cm^{-1} can be observed in both Fig. 5 b and d (left), confirming the presence of MNPs in the samples of Chit-MNPs and the PM of chitosan and MNPs. In the Chit-MNPs spectrum (Fig. 5 b (left), and Fig. 5 a-d (right)), compared to the spectra of pure chitosan (Fig. 5 a (left)) and MNPs (Fig. 5 c (left)), the 1646 cm^{-1} peak corresponding to N-H bending vibrations shifted to 1629 cm^{-1}, and the peak associated with the Fe-O bond at 544 cm^{-1} shifted to 554 cm^{-1} [29]. Electrostatic interactions between the negatively charged MNPs and positively charged chitosan led to changes in the FT-IR spectra of pure chitosan and MNPs [29] indicating that chitosan interacts with the MNP surface via nitrogen groups [30].

The FT-IR spectrum of the PM (Fig. 5 d (left)) results from the overlay of the individual spectra of the two components, preserving the amide absorption band of chitosan at 1646 cm^{-1} and the Fe-O peak of MNPs at 554 cm^{-1}.

Table 1
Properties of unmodified MNPs and chitosan modified MNPs.

Samples	Input Chit/MNPs ratio	D_{DLS} (nm)	PDI*	D_{DCS} (nm)	D_{MAG} (nm)	ZP (mV)	IEP	Chit/MNPs by TGA (mg/mg)
MNPs	–	157.5 ± 1.4	0.287	146.1	9.53 ± 0.06	+15.4 ± 1.0	6.46	–
Chit-MNPs-A	0.5	79.9 ± 0.1	0.228	72.06	8.52 ± 0.12	+27.5 ± 1.5	7.68	0.028
Chit-MNPs-B	1	91.2 ± 0.8	0.251	87.66	8.47 ± 0.11	+29.7 ± 0.6	7.75	0.035
Chit-MNPs-C	2	106.7 ± 0.9	0.268	91.86	9.02 ± 0.11	+30.8 ± 1.7	8.25	0.044
Chit-MNPs-D	3	112.9 ± 1.1	0.283	93.93	8.37 ± 0.11	+36.4 ± 0.7	9.05	0.045

*Polydispersity Index, measured by DLS.

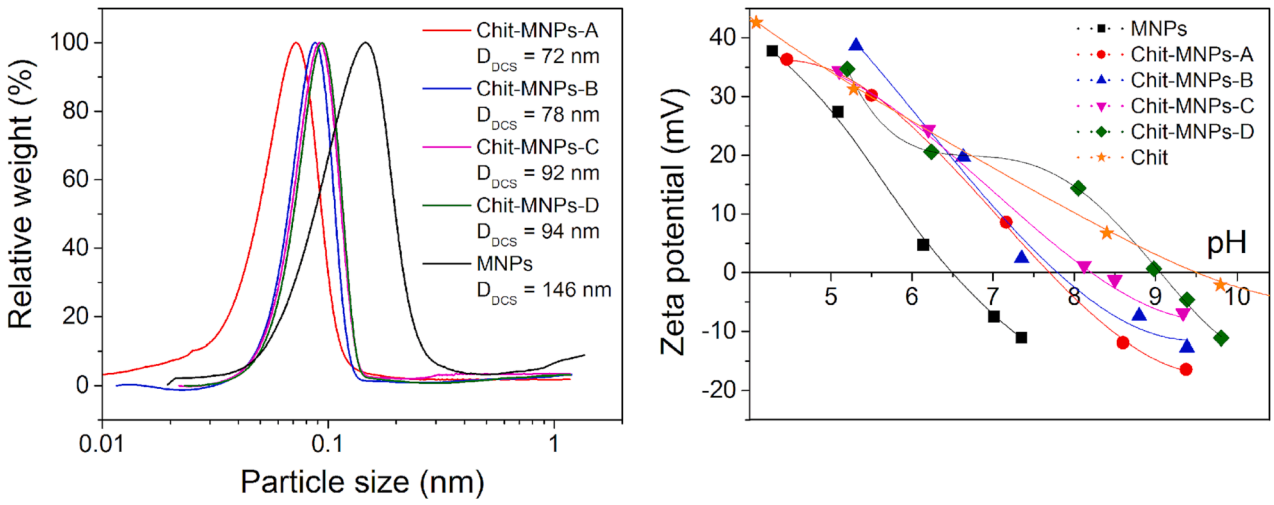

Fig. 2. Particle size distribution of MNPs and Chit-MNPs obtained from DCS measurements (left). The effect of various theoretical Chit/MNPs weight ratio on Isoelectric point (IEP), where A, B, C, and D are theoretical Chit/MNPs weight ratios of 0.5, 1, 2, and 3 w/w respectively (right).

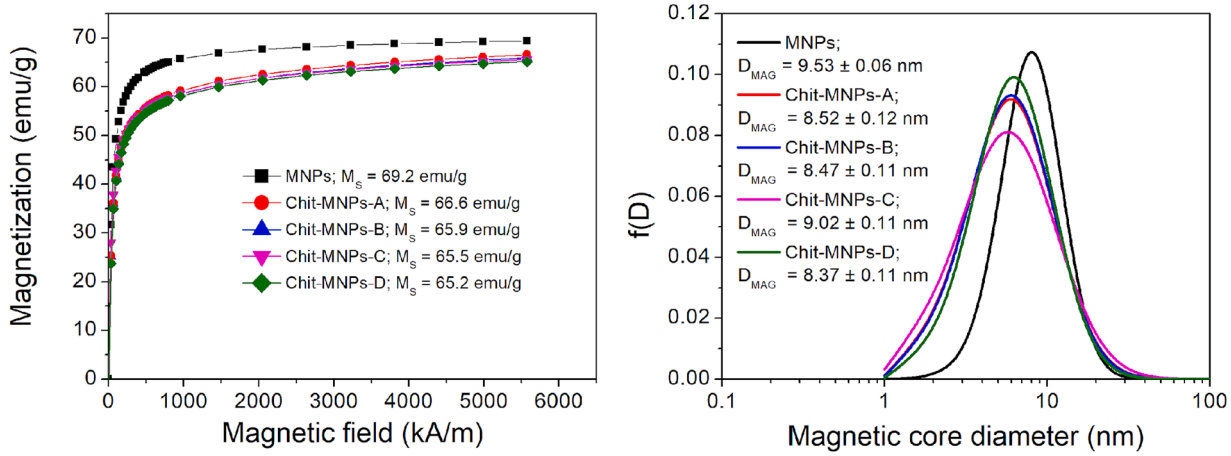

Fig. 3. Magnetization curves (left) and resulting magnetic core diameter distributions with calculated mean D_{MAG} of unmodified and chitosan modified magnetic nanoparticles at Chit/MNPs weight ratios = 0.5, 1, 2, and 3 w/w (right).

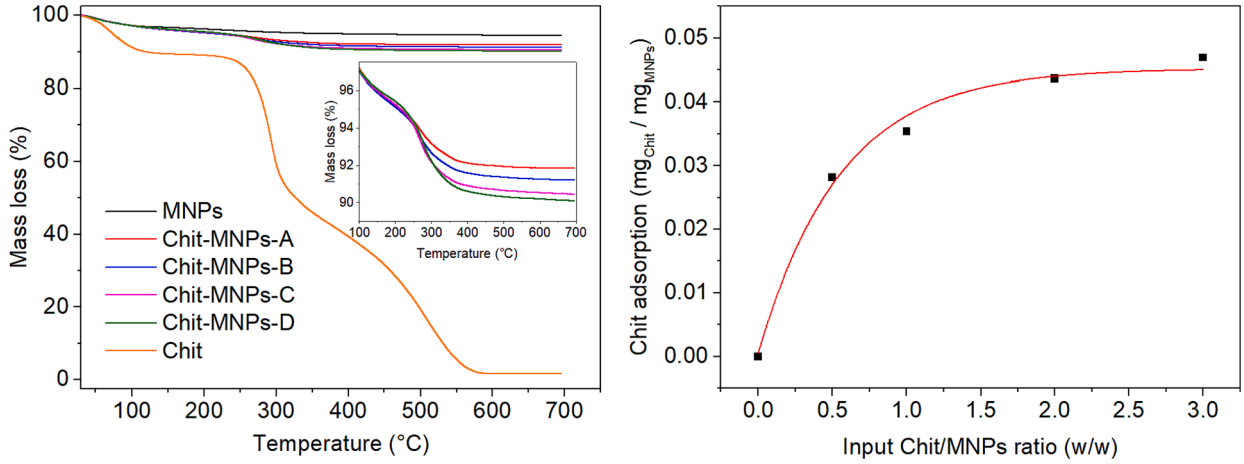

Fig. 4. TG thermograms for the samples of unmodified MNPs, pure chitosan, and chitosan modified MNPs at the chitosan to MNPs ratios of 0.5, 1, 2, and 3 w/w. The inset shows the thermograms for chitosan modified MNPs (left). Effect of chitosan adsorption on the input ratio of Chit/MNPs (right).

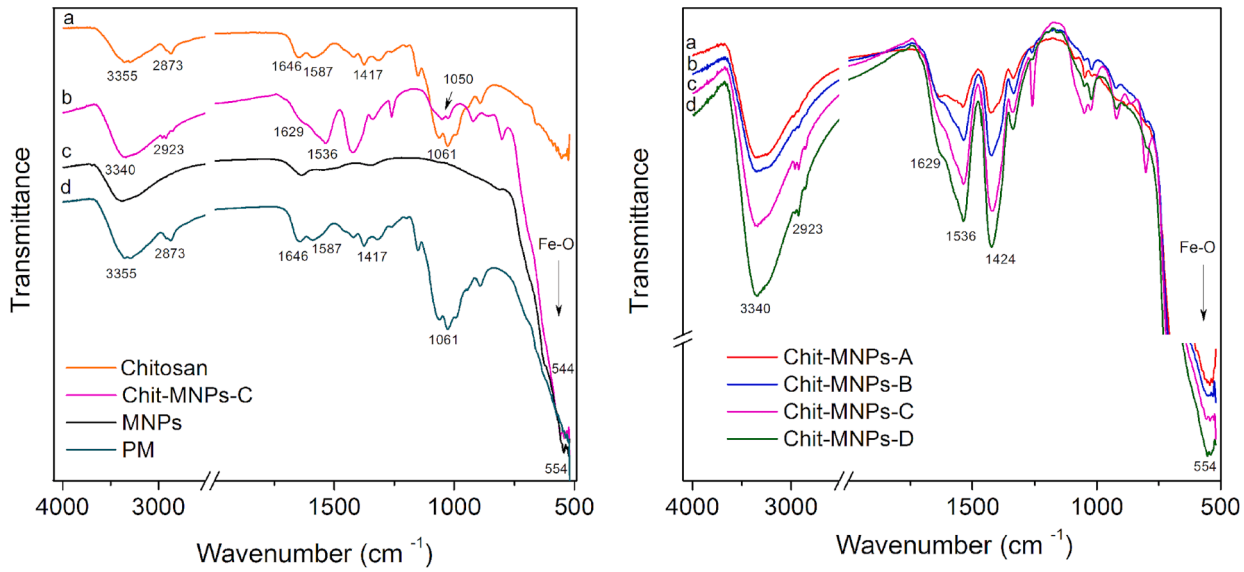

Fig. 5. FT-IR spectra of (a) pure chitosan, (b) Chit-MNPs-C, (c) unmodified MNPs, and (d) the physical mixture of chitosan and MNPs (left). FT-IR spectra of Chit-MNPs with different weight ratios of Chit/MNPs: (a) 0.5, (b) 1, (c) 2, and (d) 3 (right).

FT-IR spectra of Chit-MNPs with weight ratios of 0.5, 1, 2, and 3 (samples Chit-MNPs-A, Chit-MNPs-B, Chit-MNPs-C, and Chit-MNPs-D respectively) are presented in Fig. 5(right). In Fig. 5 (right), one can observe that the intensity of the peaks increased with the weight ratio of Chit/MNPs. This is associated with the proportion of adsorbed chitosan on the MNPs' surface. These observations indicate the successful MNPs modification by Chit.

3.2. Coating concentration dependence on peroxidase activity

The time-dependent curves and relative activity of unmodified MNPs and Chit-MNPs are shown in Fig. 6. As it can be seen, the prepared MNPs and Chit-MNPs indeed exhibited a peroxidase-like behaviour leading to DPD oxidation by hydrogen peroxide. That is, unmodified MNPs (Fe^{2+}) and DPD were respectively used as the activator of H_2O_2 to generate radical ·OH via a Fenton reaction and as the probe indicator to generate the purple-colored $DPD^{\cdot+}$ quantitatively by reacting with the generated radical ·OH [31]. In the case of Chit-MNPs, the nanoparticle surface is modified with chitosan, which is characterized by the presence of free amino groups, aminoacetyl groups, and hydroxyl groups, all of which can react with various reactive oxygen species and nitrogen species. Thereby chitosan breaks H_2O_2 leading to the formation of highly unstable oxidative species such as hydroxyl ions and free radicals [32], which in turn oxidize of DPD to the radical cation $DPD^{\cdot+}$. Thus, the absorption of the reaction solution at 551 nm as a function of reaction time for the entire range of hydrogen peroxide concentrations was used to determine the peroxide-like activity of unmodified MNPs and Chit-MNPs at different theoretical Chit/MNPs weight ratios of 0.5, 1, 2, and 3 w/w. Moreover, the relative activity of samples was determined as the ratio between the activity of Chit-MNPs and the activity of the control unmodified MNPs, which is expressed as a percentage. It was found that peroxidase activity decreases with the increase of chitosan adsorbed on the surface of MNPs (see Fig. 6 (right)).

To further elucidate the effect of chitosan concentration in samples on the peroxidase-like activity of surface modified MNPs, the absorbance data of all samples were back-calculated to concentration by the Beer-Lambert Law using a molar absorption coefficient of 43.6 M^{-1} cm^{-1} for H_2O_2-derived [33]. Apparent steady-state reaction rates at different concentrations of H_2O_2 were obtained by calculating the slopes of initial absorbance changes with time. Data shown in Fig. 7 (left) indicate that all prepared samples displayed typical Michaelis-Menten kinetics (hyperbolic kinetics), but curve characteristics varied with the different Chit/MNPs weight ratios = 0.5, 1, 2, and 3 w/w. Data were fitted (shown in Fig. 7 (left)) to the Michaelis-Menten equation and model parameters, such as V_{max} (maximum reaction rate) and K_M (the Michaelis constant) were extracted and listed in Table 2. K_M plays a role of indicator of the binding of the enzyme to the substrate, i.e., it is an indicator of strong affinity for substrates. V_{max} is catalytic velocity at the

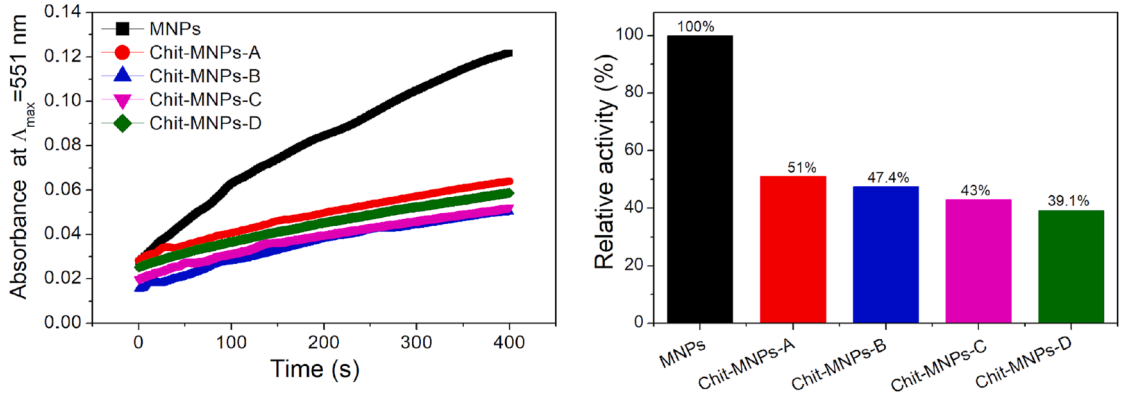

Fig. 6. Time-dependent absorbance at 551 nm (left) and relative activity (right) of MNPs and Chit-MNPs with constant concentrations of Fe_3O_4 (0.05 mg/mL), DPD (3.125×10^{-4} M), H_2O_2 ($8.0\ 10^{-3}$ M) and phosphate buffer (pH = 7.4).

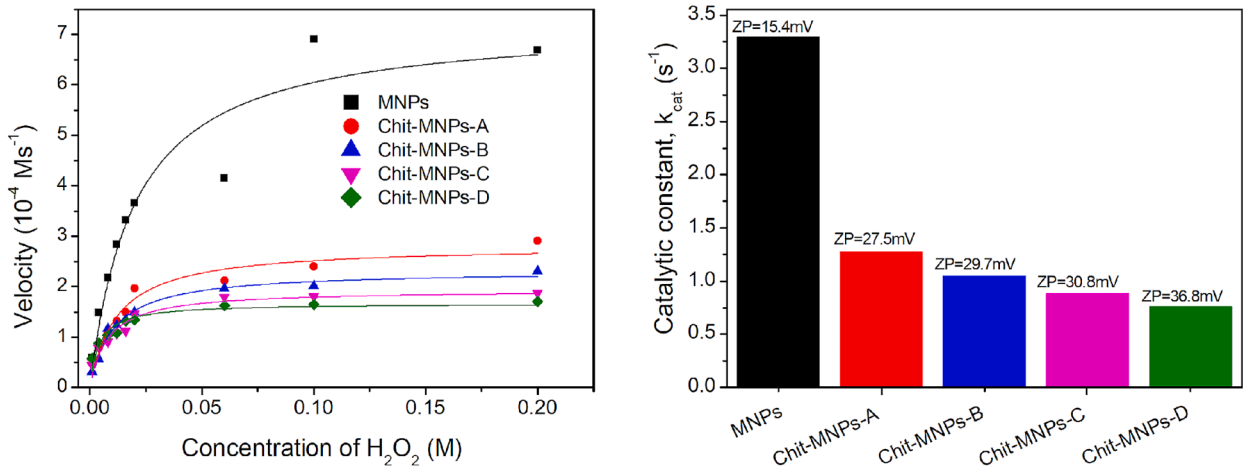

Fig. 7. Steady-state kinetic study using Michaelis-Menten model for the unmodified MNPs (black Square), Chit-MNPs-A (red Circle), Chit-MNPs-B (blue Up Triangle), Chit-MNPs-C (magenta Down Triangle) and Chit-MNPs-D (olive Diamond) with a varying concentration of H_2O_2 (left). The concentration of Fe_3O_4 (0.05 mg/mL), DPD (3.125×10^{-4} M) and phosphate buffer pH = 7.4 was the same for each reaction. Right: Catalytic constant versus zeta potential for all prepared samples (right). (For interpretation of the references to color in this figure legend, the reader is referred to the web version of this article.)

Table 2
Comparison of Michaelis-Menten parameters, optimal conditions and substrates for iron oxide MNPs activities. *Dex – Dextran, CS – Chitosan, HA – Hyaluronic acid.

Catalyst	Substrate	K_M(M)	V_{max}(Ms^{-1})	k_{cat}(s^{-1})	pH	T (°C)	Reference
MNPs	H_2O_2	10.19×10^{-3}	7.25×10^{-4}	3.39	7.4	RT	The present work
Chit-MNPs-A		11.99×10^{-3}	2.82×10^{-4}	1.28			
Chit-MNPs-B		10.37×10^{-3}	2.32×10^{-4}	1.05			
Chit-MNPs-C		7.92×10^{-3}	1.94×10^{-4}	0.88			
Chit-MNPs-D		4.03×10^{-3}	1.67×10^{-4}	0.76			
MNPs-carboxymetyl dextran	TMB	0.30×10^{-3}	1.25×10^{-7}	0.60×10^{-4}	7.4	RT	[9]
	ABTS	0.81×10^{-3}	1.15×10^{-7}	0.55×10^{-4}			
Dex@IONPs*	H_2O_2	5.95×10^{-4}	16.99×10^{-3}	–	–	RT	[18]
	TMB	3.34×10^{-8}	7.47×10^{-6}			37	
CS@IONPs*	H_2O_2	26.99×10^{-4}	2.12×10^{-3}	–	–	RT	[18]
	TMB	14.25×10^{-8}	1.62×10^{-6}			37	
HA@IONPs*	H_2O_2	7.09×10^{-4}	7.08×10^{-3}	–	–	RT	[18]
	TMB	12.55×10^{-8}	4.49×10^{-6}			37	
Horseradish peroxidase	H_2O_2	3.7	8.71×10^{-8}	3.48×10^{3}	3.5	40	[8]
	TMB	0.434	10.00×10^{-8}	4.00×10^{3}			

saturated substrate concentration and its value is also closely related to the affinity of enzyme to the substrate. Surface modification of MNPs with different Chit/MNPs weight ratio was found to affect the peroxidase-like activity of MNPs. The Chit-MNPs with theoretical Chit/MNPs weight ratios equal 0.5 and 1 w/w exhibited enhanced K_M and reduced V_{max} in comparison to the unmodified MNPs (see Table 2). The kinetic parameters K_M and V_{max} were compared with literature reported values for horseradish peroxidase (HRP). From the kinetic analysis it was found that at pH 7.4, MNPs and Chit-MNPs showed a lower activity for H_2O_2 than HRP at acidic pH (see Table 2), suggesting that MNPs require more concentration of H_2O_2 for depicting same peroxidase activity as HRP [8]. The maximum reaction velocity (V_{max}) of all samples for H_2O_2 performed at pH 7.4, obtained values (see Table 2), which was several times higher than HRP ($V_{max} = 8.71 \times 10^{-8}$ Ms^{-1}) studies reported at pH 4 [8]. It should be noted that the maximum studies of HRP are conducted at acidic pH due to limited peroxidase activity at physiological or basic pH. Therefore, the kinetic parameter values for MNPs and Chit-MNPs (at physiological pH) were compared to HRP values determined at acidic pH.

Moreover, the kinetic parameters K_M and V_{max} for Chit-MNPs were compared with literature reported parameters for polysaccharides modified iron oxide MNPs. When comparing their kinetics with that of Chit-MNPs, it was shown that K_M value for H_2O_2 was apparently higher for Chit-MNPs, indicating that polysaccharides modified iron oxide MNPs possess a lower affinity for the H_2O_2 substrate than Chit-MNPs (Table 2). Also, the maximum reaction velocity (V_{max}) of all Chit-MNPs samples for H_2O_2 was an order of magnitude lower than in the case of Dex@IONPs (Dextran coating iron oxide nanoparticles) and CS@IONPs (chitosan coating iron oxide nanoparticles) samples described in other works (see Table 2).

The catalytic constant (k_{cat}) was calculated in the following way:

$$k_{cat} = V_{max}/[E], \quad (4)$$

where $[E]$ was taken as MNPs concentration. Catalytic parameters for unmodified MNPs and Chit-MNPs were calculated and summarized in Table 2. The dependency of peroxidase activity on superficial charge are shown in Fig. 7 (right). H_2O_2 catalysis decreased rapidly with increasing ZP. Indeed, the Chit-MNPs with the strongest positive surface charge exhibited a 2.5-fold lower peroxidase activity than that in the unmodified MNPs. Hence, a higher positive charge of Chit-MNPs have greater effect on activity as suggested by the data observed for H_2O_2 in Fig. 7 (right). The catalytic constant decreases with increasing amount of adsorbed chitosan on the MNPs surface (see Table 2).

4. Conclusions

In this work, we investigated the effect of chitosan amount adsorbed on the surface of MNPs on the peroxidase-like activity of iron oxide-

based nanozyme by photometric method, which is based on the determination of low concentrations of hydrogen peroxide by the magnetic nanoparticles catalyzed oxidation of DPD. The surface of MNPs was modified by chitosan at different ratios of chitosan to MNPs. Physicochemical characterization of the synthesized samples revealed that the core of magnetic nanoparticles was roughly spherical in shape with slightly increasing hydrodynamic size with increasing input chitosan amount. Using FTIR method chitosan binding to MNPs surface was confirmed and moreover, the amount of chitosan adsorbed on MNPs surface evaluated by TGA was found to be max. 0.045 mg chitosan/mg MNPs. Finally, the relationship between the zeta potential and peroxidase-like activity was clarified. It was confirmed that unmodified MNPs and Chit-MNPs exhibit peroxidase-like activity, i.e., the ability to decompose hydrogen peroxide in the presence of substrate. We have shown that peroxidase-like activity was higher for unmodified MNPs than Chit-MNPs. The decrease in peroxidase-like activity is also aligned with indirect evidence of chitosan adsorption on the MNPs surface. Sufficiently large peroxide-like activity of chitosan modified MNPs can be utilized for diagnostic and therapeutic (anti-bacteria and cancer therapy) purposes, in organic compound detection, or in the environmental area e.g. to degrade harmful pharmaceutical ingredients present in wastewater. These results can be useful for creating sets of MNPs and Chit-MNPs samples possessing predefined peroxidase-like activity. We expect that such sets could be applicable for chromogenic reactions.

CRediT authorship contribution statement

I. Khmara: Conceptualization, Data curation, Formal analysis, Investigation, Validation, Visualization, Writing – original draft, Writing – review & editing. **I. Antal:** Formal analysis, Investigation, Validation, Visualization, Writing – original draft. **A. Jurikova:** Data curation, Formal analysis, Investigation, Validation, Visualization, Writing – original draft, Writing – review & editing. **M. Kubovcikova:** Data curation, Funding acquisition, Investigation, Project administration. **V. Zavisova:** Conceptualization, Methodology, Project administration, Resources, Software, Validation, Visualization, Writing – original draft, Writing – review & editing. **V. Girman:** Data curation, Formal analysis, Writing – original draft. **M. Koneracka:** Conceptualization, Data curation, Formal analysis, Funding acquisition, Investigation, Methodology, Project administration, Resources, Software, Supervision, Validation, Visualization, Writing – original draft, Writing – review & editing.

Declaration of competing interest

The authors declare that they have no known competing financial interests or personal relationships that could have appeared to influence the work reported in this paper.

Data availability

Data will be made available on request.

Acknowledgments

This work was supported by the Slovak Research and Development Agency under the contract no. APVV-DS-FR-22-0037; Slovak Grant Agency VEGA 02/0049/23; the Operational Program Integrated Infrastructure funded by the ERDF ITMS2014+: 313011AVG3 (BIOVID) and 3130011AUW7 (NANOVIR).

References

[1] H. Jiang, Z. Chen, C. Haiyan, Y. Huang, Peroxidase-like activity of chitosan stabilized silver nanoparticles for visual and colorimetric detection of glucose, The Analyst 137 (2012), https://doi.org/10.1039/c2an35911a.

[2] I. Khmara, et al., Chitosan-stabilized iron oxide nanoparticles for magnetic resonance imaging, J. Magn. Magn. Mater. 474 (2019) 319–325, https://doi.org/10.1016/j.jmmm.2018.11.026.

[3] C. Rümenapp, B. Gleich, A. Haase, Magnetic nanoparticles in magnetic resonance imaging and diagnostics, Pharm. Res. 29 (5) (2012) 1165–1179, https://doi.org/10.1007/s11095-012-0711-y.

[4] I. Khmara, et al., Bioactive properties of chitosan stabilized magnetic nanoparticles – Focus on hyperthermic and anti-amyloid activities, J. Magn. Magn. Mater. 513 (2020) 167056, https://doi.org/10.1016/j.jmmm.2020.167056.

[5] J. Otte, Hyperthermia in cancer therapy, Eur. J. Pediatr. 147 (6) (1988) 560–569, https://doi.org/10.1007/BF00442463.

[6] E. Kianfar, Magnetic Nanoparticles in Targeted Drug Delivery: a Review, J. Supercond. Nov. Magn. 34 (7) (2021) 1709–1735, https://doi.org/10.1007/s10948-021-05932-9.

[7] X. Mou, Z. Ali, S. Li, N. He, Applications of Magnetic Nanoparticles in Targeted Drug Delivery System, J. Nanosci. Nanotechnol. 15 (1) (2015) 54–62, https://doi.org/10.1166/jnn.2015.9585.

[8] L. Gao, et al., Intrinsic peroxidase-like activity of ferromagnetic nanoparticles, Nat. Nanotechnol. 2 (9) (2007) 577–583, https://doi.org/10.1038/nnano.2007.260.

[9] F. Yu, Y. Huang, A.J. Cole, V.C. Yang, The artificial peroxidase activity of magnetic iron oxide nanoparticles and its application to glucose detection, Biomaterials 30 (27) (2009) 4716–4722, https://doi.org/10.1016/j.biomaterials.2009.05.005.

[10] F.A. El-Essi, A.Z. Zuhri, S.I. Al-Khalil, M.S. Abdel-Latif, Spectrophotometric determination of enzymatically generated hydrogen peroxide using Sol-Gel immobilized horseradish peroxidase, Talanta 44 (11) (1997) 2051–2058, https://doi.org/10.1016/s0039-9140(97)00032-5.

[11] K.F. Fernandes, C.S. Lima, F.M. Lopes, C.H. Collins, Hydrogen peroxide detection system consisting of chemically immobilised peroxidase and spectrometer, Process Biochem. 40 (11) (2005) 3441–3445, https://doi.org/10.1016/j.procbio.2005.04.003.

[12] Y. Pan, et al., Biogenic magnetic nanoparticles from Burkholderia sp. YN01 exhibiting intrinsic peroxidase-like activity and their applications, Appl. Microbiol. Biotechnol. 99 (2) (2015) 703–715, https://doi.org/10.1007/s00253-014-5938-6.

[13] J. Wu, et al., Nanomaterials with enzyme-like characteristics (nanozymes): next-generation artificial enzymes (II), Chem. Soc. Rev. 48 (4) (2019) 1004–1076.

[14] E.S. Henle, Y. Luo, S. Linn, Fe2+, Fe3+, and Oxygen React with DNA-Derived Radicals Formed during Iron-Mediated Fenton Reactions, Biochemistry 35 (37) (1996) 12212–12219, https://doi.org/10.1021/bi961235j.

[15] W. Peng, et al., Development of chromogenic detection for biomolecular analysis, VIEW 3 (1) (2022) 20200191, https://doi.org/10.1002/VIW.20200191.

[16] Z. Chen, et al., Dual Enzyme-like Activities of Iron Oxide Nanoparticles and Their Implication for Diminishing Cytotoxicity, ACS Nano 6 (5) (2012) 4001–4012, https://doi.org/10.1021/nn300291r.

[17] H. Wei, E. Wang, Fe3O4 magnetic nanoparticles as peroxidase mimetics and their applications in H2O2 and glucose detection, Anal. Chem. 80 (6) (2008) 2250–2254, https://doi.org/10.1021/ac702203f.

[18] S.-M. You, J.-S. Park, K. Luo, K.-B. Jeong, H.J. Adra, Y.-R. Kim, Modulation of the peroxidase-like activity of iron oxide nanoparticles by surface functionalization with polysaccharides and its application for the detection of glutathione, Carbohydr. Polym. 267 (2021) 118164, https://doi.org/10.1016/j.carbpol.2021.118164.

[19] S.H. Hussein-Al-Ali, M.E. El Zowalaty, M.Z. Hussein, B.M. Geilich, T.J. Webster, Synthesis, characterization, and antimicrobial activity of an ampicillin-conjugated magnetic nanoantibiotic for medical applications, Int. J. Nanomedicine 9 (2014) 3801–3814, https://doi.org/10.2147/IJN.S61143.

[20] Z. Shen, et al., Fenton-Reaction-Acceleratable Magnetic Nanoparticles for Ferroptosis Therapy of Orthotopic Brain Tumors, ACS Nano 12 (11) (2018) 11355–11365, https://doi.org/10.1021/acsnano.8b06201.

[21] G.V. Kurlyandskaya, et al., Water-Based Suspensions of Iron Oxide Nanoparticles with Electrostatic or Steric Stabilization by Chitosan: Fabrication, Characterization and Biocompatibility, Sensors 17 (11) (2017) pp, https://doi.org/10.3390/s17112605.

[22] H. Bader, V. Sturzenegger, J. Hoigné, Photometric method for the determination of low concentrations of hydrogen peroxide by the peroxidase catalyzed oxidation of N, N-diethyl-p-phenylenediamine (DPD), Water Res. 22 (1988) 1109–1115.

[23] L. Balejčíková, K. Zelena Pospiskova, Z. Mitroova, P. Kopčanský, I. Safarik, Peroxidase-like activity of magnetoferritin, Microchim. Acta 181 (2014) 295–301, https://doi.org/10.1007/s00604-013-1105-5.

[24] G.F. Goya, H.R. Rechenberg, J.Z. Jiang, Magnetic irreversibility and relaxation in CuFe2O4 nanoparticles, J. Magn. Magn. Mater. 218 (2) (2000) 221–228, https://doi.org/10.1016/S0304-8853(00)00339-5.

[25] A. Apriceno, I. Silvestro, A. Girelli, I. Francolini, L. Pietrelli, A. Piozzi, Preparation and Characterization of Chitosan-Coated Manganese-Ferrite Nanoparticles Conjugated with Laccase for Environmental Bioremediation, Polymers 13 (9) (2021) pp, https://doi.org/10.3390/polym13091453.

[26] M.R.G. Isa Karimzadeh Mustafa Aghazadeh, Taher Doroudi, P.H. Kolivand, Electrochemical preparation and characterization of chitosan-coated superparamagnetic iron oxide (Fe3O4) nanoparticles, Mater. Res. Innov. 22 (6) (2018) 352–360, https://doi.org/10.1080/14328917.2017.1323991.

[27] M. Stoia, R. Istratie, C. Păcurariu, Investigation of magnetite nanoparticles stability in air by thermal analysis and FTIR spectroscopy, J. Therm. Anal. Calorim. 125 (3) (2016) 1185–1198, https://doi.org/10.1007/s10973-016-5393-y.

[28] Z. Bednarikova, et al., Silica-magnetite nanoparticles: Synthesis, characterization and nucleic acid separation potential, Surf. Interfaces 39 (2023) 102942, https://doi.org/10.1016/j.surfin.2023.102942.

[29] J. Safari, L. Javadian, Chitosan decorated Fe3O4 nanoparticles as a magnetic catalyst in the synthesis of phenytoin derivatives, RSC Adv 4 (90) (2014) 48973–48979, https://doi.org/10.1039/C4RA06618A.
[30] J. dos S. Menegucci, M.-K.M.S. Santos, D.J.S. Dias, J.A. Chaker, M.H. Sousa, One-step synthesis of magnetic chitosan for controlled release of 5-hydroxytryptophan, J. Magn. Magn. Mater. 380 (2015) 117–124, https://doi.org/10.1016/j.jmmm.2014.10.023.
[31] J. Zou, H. Cai, D. Wang, J. Xiao, Z. Zhou, B. Yuan, Spectrophotometric determination of trace hydrogen peroxide via the oxidative coloration of DPD using a Fenton system, Chemosphere 224 (2019) 646–652, https://doi.org/10.1016/j.chemosphere.2019.03.005.
[32] K.V. Ragavan, S.R. Ahmed, X. Weng, S. Neethirajan, Chitosan as a peroxidase mimic: Paper based sensor for the detection of hydrogen peroxide, Sens. Actuators B Chem. 272 (2018) 8–13, https://doi.org/10.1016/j.snb.2018.05.142.
[33] A.J.P.S. Mumby, R. Block, J.M.C. Gutteridge, Hydrogen peroxide and catalase are inversely related in adult patients undergoing cardiopulmonary bypass: implications for antioxidant protection, Redox Rep. 4 (1–2) (1999) 49–52, https://doi.org/10.1179/135100099101534747.